THE ASTROPHYSICAL JOURNAL, 391:137–140, 1992 May 20

SO IN STARBURST GALAXIES

S. J. PETUCHOWSKI AND C. L. BENNETT
Laboratory for Astronomy and Solar Physics, NASA Goddard Space Flight Center, MC 685, Greenbelt, MD 20771
Received 1991 October 14; accepted 1991 November 26

ABSTRACT

We describe the use of SO and SO_2 as probes of the dense interstellar medium in the nearby starburst galaxies NGC 253 and M82. Emission in the 99.3 GHz $3_2 \rightarrow 2_1$ rotational transition of SO was detected in NGC 253 and possibly in M82, and upper limits are reported for emission in the 219.9 GHz $6_5 \rightarrow 5_4$ transition of SO and two lines of SO_2. The column density of SO relative to carbon sulfide, CS, is $[N(\mathrm{SO})/N(\mathrm{CS})] > 8 \times 10^{-2}$ in NGC 253, a value not much lower than Galactic ratios and consistent with models of dense interstellar clouds (Prasad & Huntress) with a fractional abundance of atomic oxygen $\gtrsim 10^{-7}$. The 218.8 GHz $3_{21} \rightarrow 2_{20}$ transition of *para*-formaldehyde, with an excitation temperature of 68 K, was also detected in NGC 253.

Subject headings: galaxies: individual (NGC 253, M82) — galaxies: ISM — ISM: abundances — ISM: molecules

1. INTRODUCTION

Strong dependences of SO abundance on both density and cloud age are predicted by models of sulfur chemistry in interstellar clouds (Millar & Herbst 1990). Shocks are predicted to enhance the SO abundance as well, in both dense (Hartquist, Oppenheimer, & Dalgarno 1980) and diffuse (Mitchell & Deveau 1983) molecular clouds. The enhancement is compounded in the presence of an appreciable ultraviolet radiation field. Prasad & Huntress (1982) have also raised the possibility that elemental depletions might substantially affect the gas-phase chemistry of sulfur, with elemental S and Si not as severely depleted in gas that has never fully cooled. Their major conclusion is that the SO and SO_2 constitute the major repository of gas-phase sulfur in an oxygen-rich environment, while, if oxygen is depleted, most gas-phase sulfur resides in CS. For a fixed fractional abundance of sulfur of 1.7×10^{-8}, they find that the abundance of CS *decreases* from 9×10^{-9} to 4×10^{-10} as the fractional abundance of oxygen is increased from 5.5×10^{-8} to 5.5×10^{-5}, while the [SO]/[CS] ratio *increases* from 3×10^{-4} to 15 under the same conditions.

One significant difference between the *dense* ($>10^6$ cm^{-3}) molecular regions behind 4–10 km s^{-1} shocks modeled by Hartquist et al. (1980) and the *diffuse* (100 cm^{-2}) interstellar cloud subject to a 10 km s^{-1} shock explored by Mitchell & Deveau (1983) is evident in the abundance of SO_2 produced. SO is produced in both cases. In the dense case, SO is formed via reactions of atomic sulfur with O_2 and OH, attaining a fractional abundance ($\sim 4 \times 10^{-8}$) similar to that of CS. SO_2, however, is produced in abundances less than 4×10^{-11}. In the diffuse case, the high abundance of OH, especially where H_2O is exposed to UV dissociation, gives rise to the formation of greatly enhanced abundances of *both* SO and SO_2.

Sulfur monoxide is found extensively in Galactic sources. Its abundance, relative to H_2, both in quiescent regions of giant molecular clouds and in dark clouds, is typically ~ 2–5×10^{-9} (Irvine, Goldsmith, & Hjalmarson 1987). An enhancement of a factor of 300 is evident in the plateau component of Orion K-L, while SO is *under*abundant in the Orion hot core. A comparison of $N[\mathrm{SO}]/N[\mathrm{CS}]$ indicates ratios ranging from 0.2 in Sgr B2 (Irvine et al. 1987) to 23 in the Orion plateau component (Blake et al. 1987). Recent observations of Sgr B2 by Sutton et al. (1991) at higher spatial resolution suggest that SO is 2–10 times less abundant in the northern (N) maser position than in the middle (M) source.

Outside of the Milky Way, detections of both CS and SO in the Large Magellanic Cloud have recently been reported by Johansson (1991), with $\log N[\mathrm{SO}]/N[\mathrm{CS}] = 0.65 \pm 1.05$. Other observations of sulfur compounds in external galaxies have been limited to carbon sulfide, of which three radio transitions have been detected in the infrared-bright galaxies, NGC 253, M82, and IC 342 (Mauersberger & Henkel 1989, hereafter MH). Subjecting these lines to a multitransitional analysis, MH deduced CS fractional abundances, relative to H_2, consistent with the range observed in Galactic sources ($-9 < \log X(\mathrm{CS}) < -7.8$), while Nguyen-Q-Rieu, Nakai, & Jackson (1989) used CS measurements to infer a high degree of clumping in the molecular medium.

We have undertaken to determine the fractional abundance of SO in the mass of starburst galaxies associated, on the basis of maps of CS, HCN, and HCO^+ (Carlstrom 1988), with warm, ~ 50 K, and dense, $\sim 10^5$ cm^{-3}, molecular gas. Detection of the $3_2 \rightarrow 2_1$ rotational transition of SO at 99.3 GHz and limits on the $6_5 \rightarrow 5_4$ transition at 219.9 GHz constrain excitation temperature and abundance. Both M82 and NGC 253 exhibit ejection of molecular gas off the Galactic plane, presumably blown off by supernova explosions associated with an epoch of rapid star formation (Nakai et al. 1987), or O star blowouts. Both galaxies contain strong radio and far-infrared emission, and CO emission indicative of neutral molecular gas, centrally condensed in NGC 253 and in an apparent rotating torus in M82. M82, at a distance of 3.25 Mpc (Lo 1987), and NGC 253, at 3.4 Mpc (Bash et al. 1990), each exhibit ~ 40 compact radio sources that have been identified as young ($\lesssim 400$ yr) supernova remnants (Kronberg, Biermann, & Achwab 1985; Antonucci & Ulvestad 1988). The nuclear region would, presumably, reflect the chemistry of an environment replete with O and B stars and thus exposed to UV radiation that exceeds the interstellar radiation field of the Milky Way by two to three orders of magnitude (Carlstrom 1989).

The weight of observational evidence suggests a metallicity within the starburst nucleus of M82 exceeding that of Galactic giant molecular clouds by a factor of ~ 14 (Lo 1987). A high

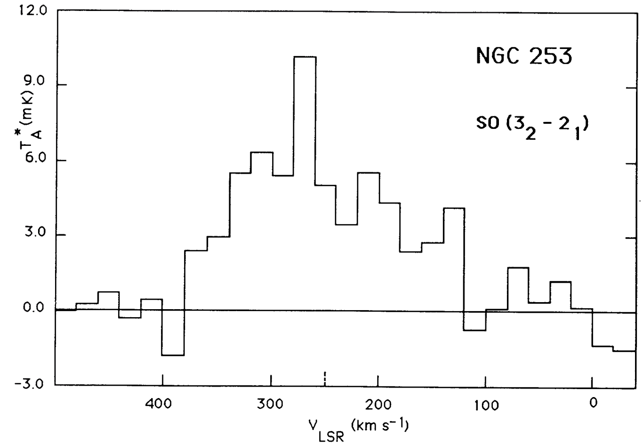

FIG. 1.—SO ($3_2 \rightarrow 2_1$) profile at 99.3 GHz toward NGC 253 ($\Delta v = 20$ km s^{-1}).

abundance of oxygen favors an excess of SO formed via ion-molecule processes involving S^+ and O_2 or OH, as discussed above. Such mechanisms actually favor formation of SO relative to CS due to the rapid reaction of CS with O to form CO + S (Blake et al. 1987). An oxygen enrichment might be expected both in winds emanating from young oxygen-rich stars and in the supernova remnants of massive stars.

2. OBSERVATIONS AND ANALYSIS

Observations were made using the NRAO[1] 12 m telescope in 1990 November and 1991 March. Two-channel SIS receivers were used at both 3 mm and 1.3 mm and were operated in single and double sideband modes, respectively.

System temperatures were typically 350–550 K for the 3 mm system and ranged from 750 to 1500 K for the 1.3 mm system. The back end employed for all observations was a bank of 256 2 MHz filters. The beamwidths at the observing frequencies of 99.3 and 219.9 GHz were 64″ and 33″, respectively. CS lines, $J = 2 \rightarrow 1$ at 97.98 GHz and $J = 5 \rightarrow 4$ at 244.9 GHz, previously detected in all the program infrared bright galaxies, were used to verify system performance and pointing, as were planets and Galactic sources.

2.1. SO

The emission spectrum of NGC 253 in the $3_2 \rightarrow 2_1$ line of SO at 99.299 GHz is shown in Figure 1. The spectrum reflects 515 minutes of integration on source and has been smoothed to a resolution of 20 km s^{-1}, for an rms of 1.3 mK. The emission line is centered at $v_{LSR} = 250$ km s^{-1}. The integrated beam temperature is $\int T(\text{SO}: 3_2 \rightarrow 2_1)dv = 1.24 \pm 0.34$ K km s^{-1}. The 219.9 GHz spectrum of NGC 253 provides a 3 σ limit of $\int T(\text{SO}: 6_5 \rightarrow 5_4)dv < 2.2$ K km s^{-1}.

Detection of the SO $3_2 \rightarrow 2_1$ line in M82, at a central position ($\alpha_{1950} = 09^h51^m42\overset{s}{.}8$; $\delta_{1950} = +69°54'59''$), is marginal. The spectrum shown in Figure 2*a* has been smoothed to a resolution of 20 km s^{-1}. The velocity centroid is 240 km s^{-1}, and the integrated beam temperature is 0.77 ± 0.4 K km s^{-1}. Our observations, similarly, provide a 3 σ limit in the SO $6_5 \rightarrow 5_4$ line of $\int T(\text{SO}: 6_5 \rightarrow 5_4)dv < 1.7$ K km s^{-1}.

[1] The National Radio Astronomy Observatory, NRAO, is operated by Associated Universities, Inc., under contract with the National Science Foundation.

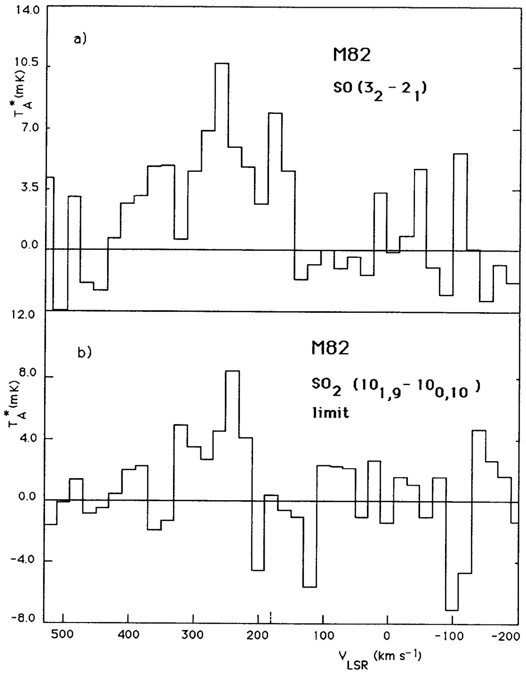

FIG. 2.—(*a*) SO ($3_2 \rightarrow 2_1$) profile at 99.3 GHz toward M82 ($\Delta v = 20$ km s^{-1}). (*b*) SO_2 ($10_{1,9} \rightarrow 10_{0,10}$) limit at 104.2 GHz, $\int T(SO_2: 10_{1,9} \rightarrow 10_{0,10})dv < 0.95$ K km s^{-1} (3 σ), toward M82 ($\Delta v = 20$ km s^{-1}).

Finally, a 3 σ limit of $\int T(\text{SO}: 3_2 \rightarrow 2_1)dv = 0.32$ K km s^{-1} is derived for the face-on Sc galaxy, IC 342, corresponding to a column limit, over the region of CO emission (comprising an estimated 74% of the beam), of $N(\text{SO}: 3_2) < 4.0 \times 10^{11}$ cm^{-2}.

2.2. SO_2

We derived limits for each of two SO_2 transitions: $3_{13} \rightarrow 2_{02}$ (104.029 GHz) and $10_{1,9} \rightarrow 10_{0,10}$ (104.239 GHz), with excitation energies of 5.38 and 30.02 cm^{-1}, respectively. The $\int T\,dv$ limits (3 σ) are identical for the two transitions. The measured $\int T\,dv$ limits and derived upper limits on column densities, in the optically thin limit, are as presented in Table 1.

The M82 spectrum at 104.2 GHz, shown in Figure 2*b*, exhibits a feature suggestive of the SO_2 $10_{1,9} \rightarrow 10_{0,10}$ line, corresponding in centroid and similar in line shape to the putative SO line at the same position. A beam-averaged column density of $N(SO_2\text{: } 10_{1,9}) = (7.0 \pm 1.3) \times 10^{11}$ cm^{-2} would be implied if the line were real and optically thin.

2.3. *Para*-H_2CO

Finally, the $3_{21} \rightarrow 2_{20}$ transition of *para*-formaldehyde was detected in NGC 253 at 218.76 GHz. The spectrum, depicted in Figure 3, is characterized by a centroid of 230 km s^{-1}, and an integrated intensity of 2.0 K km s^{-1}. Detection in nearby galaxies of rotational transitions of *para*-H_2CO was anticipated

TABLE 1

SO_2 DETECTION LIMITS (3 σ)

Source	$\int T\,dv$ (K km s^{-1})	$N(SO_2\text{: }3_{13})$ (cm^{-2})	$N(SO_2\text{: }10_{1,9})$ (cm^{-2})
NGC 253	<2.14	$<4.5 \times 10^{13}$	$<4.0 \times 10^{13}$
M82	<0.95	$<2.0 \times 10^{12}$	$<1.8 \times 10^{12}$

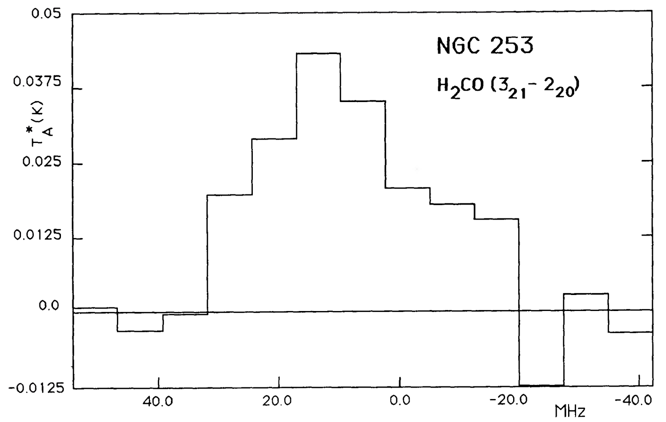

FIG. 3.—H_2CO ($3_{21} \rightarrow 2_{20}$) profile at 218.8 GHz toward NGC 253 ($\Delta v = 10$ km s^{-1}). The frequency is relative to $v_{LSR} = 250$ km s^{-1}.

by Baan et al. (1990) in connection with their detection, in M82, of the $3_{03} \rightarrow 2_{02}$ transition at 218.22 GHz.

3. DISCUSSION AND CONCLUSIONS

3.1. *Implications of* SO *and* CS *Measurements*

We apply a bootstrap technique to derive column densities, since morphologies and optical depths are unknown, a priori. We have made the useful assumption that emission by SO and CS is coextensive, on the grounds that their rotational dipole moments are comparable ($\mu_{SO} = 1.55$ D; $\mu_{CS} = 1.97$ D) and they are thus excited collisionally under similar ($n \gtrsim 10^4$ cm^{-3}) conditions, although there are shock scenarios discussed in the Introduction which could account for extreme chemical differentiation. We have also assumed that SO and CS are rotationally equilibrated. Note that we need not require local thermal equilibrium but only that the same T_{rot} characterizes the SO $3_2 \rightarrow 2_1$ and CS $2 \rightarrow 1$ transitions whose excitation energies are 2.933 cm^{-1} and 4.902 cm^{-1}.

The optical depth τ of a transition is proportional to the quantity:

$$\tau \sim \mu^2 S N_k [g_l/g_u](1 - e^{-h\nu/kT}) , \quad (1)$$

where g_k is the M-degeneracy of the upper and lower state, ν is the transition frequency, and S is the transition strength, $S \equiv (2J_u + 1)\langle \mu_{ij} \rangle^2/\mu^2$, as conventionally defined, and N_k is the state-specific column density of the upper level of the transition. Under the conditions we have assumed,

$$\frac{\tau_{SO\,(99\,GHz)}}{\tau_{CS\,(98\,GHz)}} = 1.08\Phi(T) \frac{N[SO\ 3_2]}{N[CS\ J = 2]} , \quad (2)$$

where the temperature dependence is conveyed by $\Phi(T)$.

We further assume $T_{rot} = 50$ K as a nominal value for both sources. Telesco & Harper (1980) find a dust color temperature of 40 K in NGC 253 (45 K in M82), although there is also ample evidence for small, hot grains (Telesco 1991). The temperature is not tightly constrained by the analysis of MH who adopt $T = 60$ K for calculational purposes, and our result is also insensitive to temperature. In fact, $\Phi(T = 50\ K) = 1.01$, and $\Phi(T)$ varies less than 1% between 30 and 70 K.

In NGC 253, we derive an optical depth of $\tau = 2.25$ (+0.7, −0.6) in the $J = 2 \rightarrow 1$ CS line by comparing the ratio, as reported by MH, $W(C^{32}S)/W(C^{34}S) = 9.2 \pm 1.5$, with an abundance ratio assumed equal to the terrestrial value of 23.

The column density in the emitting (upper) state of a molecule can be expressed in terms of observables as

$$N_k = \frac{3kg_k W}{8\pi^3 \mu^2 \nu S} \frac{\tau}{1 - e^{-\tau}} , \quad (3)$$

where $W \equiv \int T_b dv$ is the line integrated main beam temperature, and the correction for escape probability is expressed in terms of the optical depth. To account for the extent of the emitting region, we have convolved the 3 mm beam ($\theta_b = 64''$) with the $39'' \times 12''$ angular extent of the molecular bar mapped by Canzian, Mundy, & Scoville (1988) in CO, and we derive a beam filling factor $f = \theta_{maj}\theta_{min}/(\theta_{maj}\theta_{min} + \theta_b^2) = 0.10$ at 99.3 GHz. At 219.9 GHz, a small fraction of the emitting region falls outside the FWHM of the beam, while we assume that the Gaussian beam is filled by $\sim$0.46. It is likely that we are overestimating the size of the emission region since critical densities in SO probably exceed those of CO by two orders of magnitude. There is also evidence in Sgr B2 that SO emission is more localized than CS emission (Goldsmith et al. 1987; Sutton et al. 1991). Solution of equations (2) and (3) yields the optical depth in the SO $3_2 \rightarrow 2_1$ line, $\tau_{SO\,(99\,GHz)} = 0.15$ (+0.15, −0.07). Applying beam and opacity corrections leads to a column density, averaged over the angular dimensions of the molecular bar, of $N(SO: 3_2) = (2.2 + 1.0, -0.7) \times 10^{13}$ cm^{-2}.

The ratio of the optical depth of the SO $6_5 \rightarrow 5_4$ transition at 219 GHz to the 99 GHz transition is a function of temperature, plotted in Figure 4, and equal to 2.87 at 50 K. The ratio of SO level populations, between 6_5 at an excitation energy of 24.32 cm^{-1} and 3_2 at 6.41 cm^{-1}, is

$$\frac{N(6_5)}{N(3_2)} = 0.41 \frac{W(219)\beta(99)}{W(99)\beta(219)} , \quad (4)$$

where $\beta = (1 - e^{-\tau})/\tau$ is the photon escape probability. In rotational equilibrium, $N(6_5)/N(3_2) = 13/7 \exp(-25.8/T_{rot}) = 1.11$ at $T_{rot} = 50$ K.

Our 3 σ limit at 219.9 GHz, corrected for beam filling, corresponds to $W(219)/W(99) < 0.39$. This implies that no more than 16% of the SO detected at 99 GHz can be characterized by a rotational temperature as warm as 50 K. The highest rotational temperature characterizing the entire column of SO is $T_{rot} = 15$ K, in which case the overall column density of SO

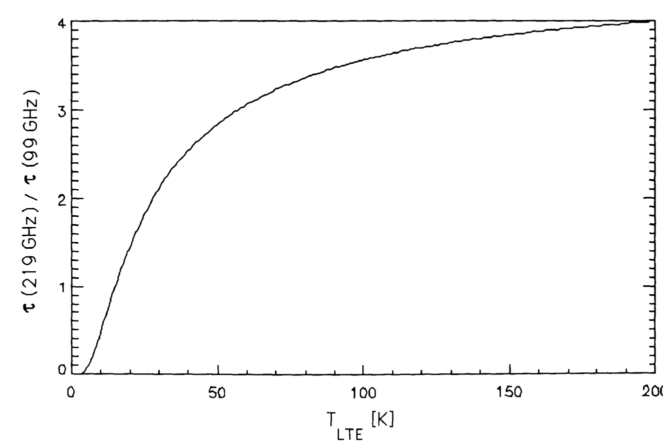

FIG. 4.—Calculated ratio of SO rotational line opacities, $\tau(219)/\tau(99)$ vs. T

would be 2.9×10^{14} cm^{-2}. This is a lower limit since a large column could be present at a lower rotational temperature.

The spectral proximity of the CS $2 \rightarrow 1$ line at 97.98 GHz to the 99 GHz SO line allows us to determine a column density over substantially the same region. Applying corrections for beam filling and optical opacity to the measurement of $\int T(\mathrm{CS}: 2 \rightarrow 1)dv = 13.1 \pm 5.4$ K, we derive a column density in NGC 253 of $N(\mathrm{CS}: J = 2) = (3.6 \pm 2.2) \times 10^{14}$ cm^{-2}. A thermal distribution of CS characterized by $T_{\mathrm{rot}} = 50$ K implies an overall CS column density of 3.5×10^{15} cm^{-2}. The resultant abundance ratio, $N(\mathrm{SO})/N(\mathrm{CS}) > 8 \times 10^{-2}$, is, at most, a factor of 3 lower than the Sgr B2 value, despite apparently radically different global properties of the galactic medium.

In M82, a column density of $N(3_2) = (1.3 \pm 0.5) \times 10^{12}$ cm^{-2}, averaged over the beam, is inferred from the 99 GHz measurement, in the optically thin case. The 219 GHz limit cannot provide a meaningful excitation limit owing to the complex morphology of the source. In rotational equilibrium, at most 17% of the SO is in the 3_2 rotational state. We can thus infer a total SO column of greater than 7.6×10^{13} cm^{-2}. Comparison with the CS column of 1.0×10^{15} cm^{-2} reported by MH leads to an abundance ratio of greater than 8×10^{-2}, identical to that in NGC 253. The limit in IC 342, $N(\mathrm{SO})/N(\mathrm{CS}) < 0.4$, is consistent with the other sources.

3.2. *Implications of* SO_2 *and* SO

Even if both SO and SO_2 lines are present in the M82 spectra of Figure 2, a meaningful comparison of abundances is impossible until other transitions of both species are detected. The emission of these species in Sgr B2, for example, is characterized by very different rotational temperatures. The upper level of the detected $3_{21} \rightarrow 2_{20}$ transition has an excitation temperature of 68.1 K. The collisional de-excitation rate of Green et al. (1978) and stimulated emission coefficient of Jaruschewski et al. (1986) imply a critical density of 5.3×10^6 cm^{-3} for the transition. Thus, if collisionally excited, this line implies the presence of warm, dense gas. An assumption of $T_{\mathrm{rot}} \approx 50$ K for SO_2 implies $N(SO_2) = (4.0 \pm 0.7) \times 10^{13}$ cm^{-2}, and $[N(SO_2)/N(\mathrm{SO})] < 0.5$. This is similar to Galactic sources (Irvine et al. 1987) and would preclude SO formation according to the shocked dense medium scenario.

3.3. *Implications of para*-H_2CO

Applying the beam correction of 46%, as discussed above, we derive a column density in the emitting *para*-H_2CO 3_{21} state of 2.6×10^{10} cm^{-2}, averaged over the molecular bar. Comparing this column density with the average hydrogen column density of 3×10^{22} cm^{-2} (Canzian et al. 1988), and recognizing that the thermal equilibrium fraction of 0.018 of *para*-formaldehyde ($T = 50 \pm 10$ K) constitutes an upper limit, we derive a lower limit to the fractional abundance of *para*-formaldehyde of $N[\textit{para}\text{-formaldehyde}]/N[H_2] > 5 \times 10^{-11}$. If the *para*-formaldehyde abundance represents a statistical fraction, $\frac{1}{4}$, of the total formaldehyde abundance, then the fractional abundance represented by *warm* formaldehyde is greater than 2×10^{-10}. If the overall formaldehyde abundance is comparable to Galactic values, $\sim 10^{-9}$ at $n(H_2) \sim 10^5$ cm^{-3} (Wadiak, Rood, & Wilson 1988), this indicates that an appreciable fraction ($>20\%$) of the molecular material represented by the CO emission measured by Canzian et al. (1988) is warm gas.

3.4. *Summary*

1. Sulfur monoxide has been detected in one, possibly two, new extragalactic sources, both nearby starburst galaxies.
2. The abundance relative to CS is not substantially lower than Galactic values, and corresponds to at least an intermediate ($\gtrsim 10^{-7}$) fractional abundance of oxygen in the Prasad & Huntress (1982) model.
3. The abundance of SO_2, if present in M82, is not dissimilar from Galactic values, and would preclude formation of SO in shocked dense clouds.
4. The newly detected 218 GHz formaldehyde $3_{21} \rightarrow 2_{20}$ line indicates the presence, in NGC 253, of substantial highly excited molecular material.

We gratefully acknowledge the assistance provided by Phil Jewell and the NRAO Tucson staff.

REFERENCES

Antonucci, R. R. J., & Ulvestad, J. S. 1988, ApJ, 330, L97
Baan, W. A., Henkel, C., Schilke, P., Mauersberger, R., & Güsten, R. 1990, ApJ, 353, 132
Bash, F. N., Davis, J. H., Jaffe, D. T., Wall, W. F., & Sutton, E. C. 1990, in Submillimetre Astronomy, ed. G. D. Watt & A. S. Webster (Dordrecht: Kluwer), 227
Blake, G. A., Sutton, E. C., Masson, C. R., & Phillips, T. G. 1987, ApJ, 315, 621
Canzian, B., Mundy, L. G., & Scoville, N. Z. 1988, ApJ, 333, 157
Carlstrom, J. E. 1988, in Galactic and Extragalactic Star Formation, ed. R. E. Pudritz & M. Fich (Dordrecht: Kluwer), 571
———. 1989, Ph.D. dissertation, University of California, Berkeley
Goldsmith, P. E., Snell, R. L., Hasegawa, T., & Ukita, N. 1987, ApJ, 314, 525
Green, S., Garrison, B. J., Lester, W. A., Jr., & Miller, W. H. 1978, ApJS, 37, 321
Hartquist, T. W., Oppenheimer, M., & Dalgarno, A. 1980, ApJ, 236, 182
Irvine, W. M., Goldsmith, P. F., & Hjalmarson, Å. 1987, in Interstellar Processes, ed. D. J. Hollenbach & H. A. Thronson, Jr. (Dordrecht: Reidel), 561
Jaruschewski, S., Chandra, S., Varshalovich, D. A., & Kegel, W. H. 1986, A&AS, 63, 307
Johansson, L. E. B. 1991, in Dynamics of Galaxies and Their Molecular Cloud Distributions, ed. F. Combes & F. Casoli (Dordrecht: Kluwer), 1
Kronberg, P. P., Biermann, P., & Achwab, F. R. 1985, ApJ, 291, 693
Lo, K. Y. 1987, in Star Formation in Galaxies, ed. C. J. Lonsdale Persson (NASA CP 2466), 367
Mauersberger, R., & Henkel, C. 1989, A&A, 223, 79 (MH)
Millar, T. J., & Herbst, E. 1990, A&A, 231, 466
Mitchell, G. F., & Deveau, T. J. 1983, ApJ, 266, 646
Nakai, N., Hayashi, M., Handa, T., Sofue, Y., Hasegawa, T., & Sasaki, M. 1987, PASJ, 39, 685
Nguyen-Q-Rieu, Nakai, N., & Jackson, J. M. 1989, A&A, 220, 57
Prasad, S. S., & Huntress, W. T., Jr. 1982, ApJ, 260, 590
Sutton, E. C., Jaminet, P. A., Danchi, W. C., & Blake, G. A. 1991, ApJS, 77, 255
Telesco, C. M. 1991, ApJ, 343, L13
Telesco, C. M., & Harper, D. A. 1980, ApJ, 235, 392
Wadiak, E. J., Rood, R. T., & Wilson, T. L. 1988, ApJ, 324, 931